Tracking performance studies for the Experimental Setup at the Electron-Ion Collider

Shyam Kumar[1,3,*], *Annalisa* Mastroserio[2,3], and *Domenico* Elia[3]

[1]Università degli Studi di Bari Aldo Moro, Italy
[2]Università degli Studi di Foggia, Italy
[3]INFN, sezione di Bari, Italy

Abstract. The US Electron-Ion Collider (EIC) is a future facility to be built at the Brookhaven National Laboratory (BNL) to study the collisions of polarized electrons with polarized protons and ions. It will provide the answers to fundamental questions on quark and gluon interactions such as: how colored partons and colorless jets travel in the nuclear medium, the properties of the state of matter in high gluon density (low-x) regime, distribution of quarks, gluons, and their spin inside a nucleon. EIC is expected to run at the luminosity of 10^{32}-10^{34} cm^{-2} sec^{-1} and center-of-mass energy 20-140 GeV [1]. ATHENA (A Totally Hermetic Electron Nucleus Apparatus) is one of the detector designs provided as the response to the call for the proposal issued by the EIC Project in 2021. It consists of a tracking system with wide pseudorapidity coverage ($|\eta|<3.5$), high granularity (pixel size of inner layers ~10 μm), and low material budget (0.05% of X_0 per layer) for the innermost silicon layers to achieve good tracking and vertexing performances.

1 Introduction

ATHENA is one of the experimental designs proposed for experiments at the US EIC, providing the basis for the further optimization of tracking and vertexing performance currently ongoing. Within this context, we performed the simulation in Fun4All [2] and Detector Description Toolkit for High Energy Physics (DD4hep) [3] frameworks. We first simulate a single particle using an event generator uniform in pseudorapidity (η) and momentum then transport it to the detector material using a particle gun in GEANT4 [4]. The dedicated full digitization and hit reconstruction is performed considering the response of each detector. After the hit reconstruction, tracking is performed using a Kalman filter to estimate the tracking performance of the detector system. The tracking performances are given by the momentum resolution and distance of closest approach (DCA) resolution [5,6]. The momentum resolution affects the RMS of invariant mass spectra of the identified particles and DCA resolution is very important for the reconstruction of secondary particles mostly originated by the weak decays of particles that decay close to the interaction point, e.g. D^0 meson ($c\tau$ = 123 μm). In this paper, we present the study of tracking performances

*e-mail: shyam.kumar@ba.infn.it

of the ATHENA detector [7] in each η bin and compare them with the requirements dictated by the physics goals of the experiment.

2 Design of the Tracker

The ATHENA tracker consists of detectors in the central region, forward region, and the backward region as shown in Fig. 1 and detailed in the following sections.

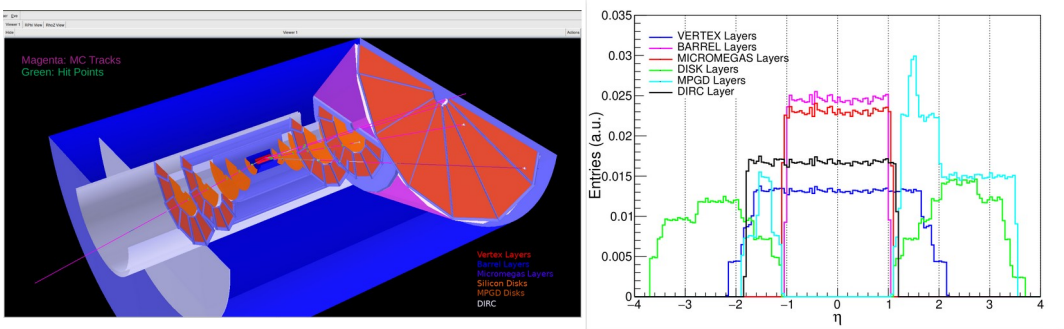

Fig. 1. (Left) Event Display of ATHENA showing the detector volumes with embedded pion MC tracks (magenta) and hits (green) using Fun4All simulation framework; (Right) Pseudorapidity coverage for each detector from the hit points on the detector surface.

1. Central Tracker

The central part of the ATHENA tracking system consists of three vertex layers and two barrel sagitta layers based on silicon Monolithic Active Pixel Sensors (MAPS) in 65 nm CMOS technology currently being developed by the ALICE Collaboration for the upgrade of the inner tracking system in view of Run 4 (ITS3): a schematic picture of the ALICE ITS3 system is shown in Fig. 2. Each of the silicon vertex layers consists of pixel cells with a size ~ 10 μm. It also consists of four micromegas layers with a resolution of $\sigma_{r\varphi} = \sigma_z =$ 150 μm. The innermost layers of silicon sensors with an extremely small material budget and excellent spatial resolution will be key for achieving the physics requirements. The configuration details of the central tracking layers are described in Tables 1, 2, and 3.

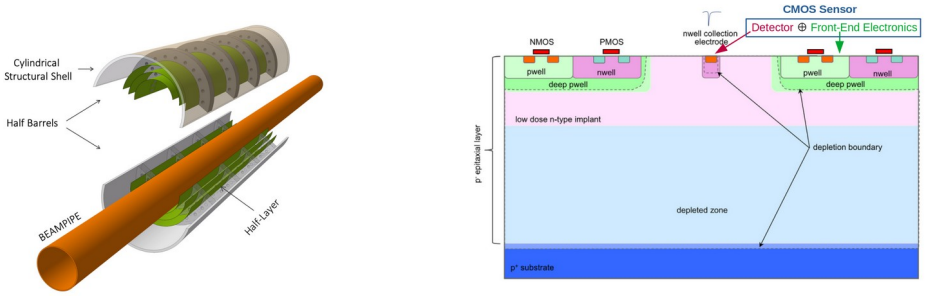

Fig. 2. (Left) The layout of the ALICE ITS3 detector [8]; (Right) ALICE ITS3 MAPS Sensor [9].

Table 1. The geometric parameters of Silicon Vertex Layers [10].

Radius (cm)	Length (cm)	Pixel Pitch	(X/X_0 %)
3.3	28.0	10 μm	0.05
4.35	28.0	10 μm	0.05
5.4	28.0	10 μm	0.05

Table 2. The geometric parameters of Silicon Barrel (Sagitta) Layers [10].

Radius (cm)	Length (cm)	Pixel Pitch	(X/X_0 %)
13.34	34.34	10 μm	0.55
17.96	46.68	10 μm	0.55

Table 3. The geometric parameters of Micromegas Barrel Layers [10].

Radius (cm)	Length (cm)	Resolution	(X/X_0 %)
47.72	127.47	150 μm ($\sigma_{r\varphi}$) x 150 μm (σ_z)	0.4
49.57	127.47	150 μm ($\sigma_{r\varphi}$) x 150 μm (σ_z)	0.4
75.61	201.98	150 um ($\sigma_{r\varphi}$) x 150 μm (σ_z)	0.4
77.46	201.98	150 μm ($\sigma_{r\varphi}$) x 150 μm (σ_z)	0.4

2. Forward and Backward Tracker

In the forward region, the ATHENA tracker consists of six silicon disks (X/X_0 = 0.24% per layer) with a pixel cell size ~ 10 μm, while in the backward region five silicon disks with the similar pixel size and material budget. The two outer silicon disks in the forward and backward region are complemented by the micro-pattern gaseous detector (MPGD) layers to avoid the acceptance gap while moving from the barrel to the forward or backward region. The setup also has an MPGD layer in the most forward region. The MPGD layers have the material budget (X/X_0 = 0.4% per layer) and spatial resolution σ_r = 250 μm, $\sigma_{r\varphi}$ = 50 μm. The configuration details of the forward and backward tracking layers are described in Tables 4 and 5.

Table 4. The geometric parameters of Forward and Backward Silicon Disks [10].

Six Forward Silicon Disks			5 Backward Silicon Disks		
R_{in} (cm)	R_{out} (cm)	Z (cm)	R_{in} (cm)	R_{out} (cm)	Z (cm)
3.18	18.62	25.0	3.18	18.62	-25.0
3.18	36.50	49.0	3.18	36.50	-49.0
3.47	43.23	73.0	3.18	43.23	-73.0
5.08	43.23	103.65	3.95	43.23	-109.0
6.58	43.23	134.33	5.26	43.23	-145.0
8.16	43.23	165.0			

Table 5. The geometric parameters of Forward and Backward MPGD Layers [10].

Forward MPGD Layers			Backward MPGD Layers		
R_{in} (cm)	R_{out} (cm)	Z (cm)	R_{in} (cm)	R_{out} (cm)	Z (cm)
44.68	76.91	105.76	44.68	76.91	-103.0
44.68	76.91	161.74	44.68	76.91	-141.74
19.34	195.5	332.0			

3 Simulation Results

To understand the performance of the tracking system negative pions were simulated and their transport to the detector material was done using GEANT4. After simulation, digitization, hit reconstruction, and tracking was performed within the framework. We evaluated the momentum resolution as a function of momentum, and DCA in the transverse plane as a function of transverse momentum in different η intervals as shown in Fig. 3 and 4. The green points are extracted from the full detector simulations, the orange curve corresponds to the results of the fit to the data points, and the blue curve represents the physics requirements as shown in Table 6.

The uncertainty in the momentum measurement comes from two sources: the finite size of pixels, namely the spatial resolution (S.R.), and the thickness of the detector material, which impacts on the multiple scattering (M.S.), experienced by the particles crossing it. These effects at $\eta = 0$ can be parameterized for the detector planes with equal spatial resolutions, spacing, and equal thickness (Gluckstern approach) with the following expressions [5,6] :

$$\left(\frac{\sigma_p}{p}\right)_{SR} \approx \frac{\sigma_{r\varphi} p}{0.3 B L^2}\sqrt{\frac{720}{N+5}} \qquad \left(\frac{\sigma_p}{p}\right)_{MS} \approx \frac{0.0136 GeV/c}{0.3 \beta B L}\sqrt{\frac{d_{total}}{X_0}} \qquad \left(\frac{\sigma_p}{p}\right) = \sqrt{\left(\frac{\sigma_p}{p}\right)_{SR}^2 + \left(\frac{\sigma_p}{p}\right)_{MS}^2}$$

where p, $\sigma_{r\varphi}$, B, β, d_{total}, X_0, and L represent momentum, spatial resolution of the detector, magnetic field, velocity, total thickness of detector, radiation length of the traversed material, and the lever arm (distance between first and the last layer of setup) of the detector setup, respectively.

Momentum resolution due to spatial resolution varies linearly with momentum for which the slope can be reduced by increasing the number of detector planes (N), by decreasing the spatial resolution, and by increasing the magnetic field and lever arm. The momentum resolution due to multiple scattering stays constant except at low momentum where there is an increase because of the lower value of beta at low momentum. The constant term can be reduced by increasing the product between the magnetic field and lever arm (B*L) but that will also increase d_{total}. Therefore, we need to balance between two terms S.R. and M.S. to achieve an optimal detector design to minimize the uncertainty in the momentum measurement. The analytical expression used for the fit ($f(dp/p)=\sqrt{A^2 p^2 + B^2}$) of the momentum resolution curves obtained by the ATHENA simulation studies consists of two terms: the first one (M.S.) is considered to be constant after neglecting the low momentum regime ($\beta<1$) while the other (S.R.) is linear in momentum.

The transverse DCA resolution (DCA_{xy} or DCA_T) also consists of two similar terms associated with S.R. and M.S. respectively, as appears from the following formulas [5,6]:

$$(\sigma DCA_{xy})_{SR} \approx \frac{3\sigma_{r\phi}}{\sqrt{N+5}}\sqrt{1+8\frac{r_0}{L}+28\frac{r_0^2}{L^2}+40\frac{r_0^3}{L^3}+20\frac{r_0^4}{L^4}}$$

$$(\sigma DCA_{xy})_{MS} \approx 0.0136 GeV/c \frac{r_0}{\beta p_T}\sqrt{\frac{d}{X_0 \sin\theta}}\sqrt{1+\frac{1}{2}\left(\frac{r_0}{L}\right)+\frac{N}{4}\left(\frac{r_0}{L}\right)^2} \qquad \sigma DCA_{xy} = \sqrt{(\sigma DCA_{xy})_{SR}^2+(\sigma DCA_{xy})_{MS}^2}$$

In the case of DCA_{xy} resolution, the S.R. terms stay constant with p_T. It can be reduced by decreasing spatial resolution, increasing the number of layers, and putting the first layer very close to the interaction point (r_0 radius of the first layer). The multiple scattering term decreases with momentum because of the $1/p_T$ term: it can be further be decreased by reducing r_0 and the thickness of sensors. Therefore, the ATHENA fit ($f(DCA_T)=\sqrt{A^2/p_T^2+B^2}$) for the DCA_{xy} resolution also consists of two terms, one constant (S.R.) and the other proportional to the inverse of momentum (M.S.). The tracking performances met the physics requirements as stated in the Yellow Report (YR) [1], except for the most backward -3.5 < η < -2.5 and momenta below 2 GeV, respectively. Further technology R&D to reduce material, combined with sophisticated analysis techniques and further overall detector layout optimizations will be needed to fully achieve the EIC physics goals.

Table 6. Physics requirements on tracking in different bins [1].

Acceptance	Momentum Resolution σ(p)/p		DCA_T Resolution	
	Performances	Requirements	Performances	Requirements
-3.5 < η< -2.5	~ 0.04%×p ⊕1.5 %	~ 0.1%×p ⊕0.5 %	~ 80/p_T ⊕10 μm	~ 30/p_T ⊕50 μm
-2.5 < η< -1.0	~ 0.01%×p ⊕ 0.5 %	~ 0.05%×p ⊕ 0.5 %	~ 50/p_T ⊕5 μm	~ 30/p_T ⊕20 μm
-1.0 < η< 1.0	~ 0.05%×p ⊕ 0.4 %	~ 0.05%×p ⊕ 0.5 %	~ 30/p_T ⊕5 μm	~ 20/p_T ⊕5 μm
1.0 < η< 2.5	~ 0.01%×p ⊕ 0.5 %	~ 0.05%×p ⊕ 1.0 %	~ 50/p_T ⊕5 μm	~ 30/p_T ⊕20 μm
2.5 < η< 3.5	~ 0.02%×p ⊕ 1.5 %	~ 0.1%×p ⊕ 2.0 %	~ 80/p_T ⊕10 μm	~ 30/p_T ⊕50 μm

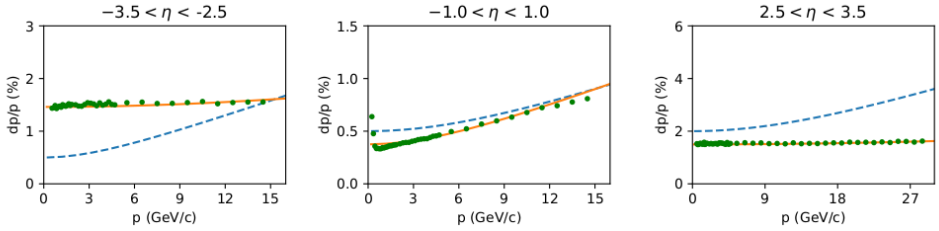

Fig. 3. Momentum resolutions versus momentum for the ATHENA setup corresponding to simulated pions- uniform in η momentum compared to the physics requirements in YR for selected η bins [7].

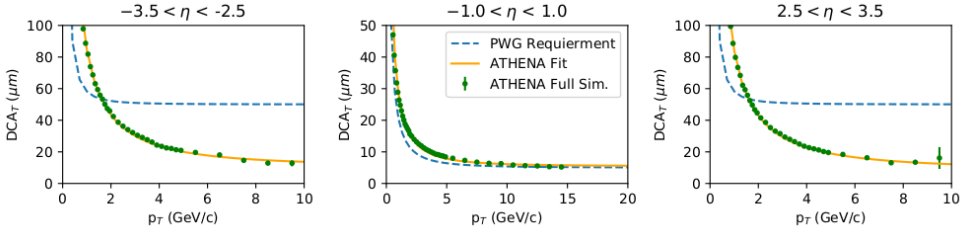

Fig. 4. Transverse DCA resolutions versus transverse momentum for the ATHENA setup corresponding to simulated pions- uniform in η momentum compared to the physics requirements in YR for selected η bins [7].

4 Conclusions

EIC is a future facility with unique physics programme due to its unique characteristics (e.g. energy, luminosity, polarized beams). It will require an excellent tracking detector system that can reconstruct particles produced in the collision with very small uncertainties. As described above, we performed the full simulation of the ATHENA tracker in Fun4All and DD4hep simulation frameworks. The tracking performances are estimated using the above geometry and the physics requirement are satisfied everywhere except that in few η bins where the tracker configuration still needs to be optimized both in geometry and material budget. The EIC community is currently working in Electron Proton Ion Collider (EPIC) collaboration with the aim of combining the existing studies performed for the detector proposals in 2021 (including ATHENA) and preparing a baseline detector configuration in view of the technical design report (TDR) activities in 2023.

References

1. R. Abdul Khalek, *et al.,* Science Requirements and Detector Concepts for the Electron-Ion Collider*: EIC Yellow Report,* Nucl. Phys. A **1026**, 122447 (2022)
2. Fun4All, https://wiki.bnl.gov/sPHENIX/index.php/EIC_SPHENIX_FUN4ALL
3. M. Frank, F. Gaede, C. Grefe and P. Mato, DD4hep: DD4hep: A Detector Description Toolkit for High Energy Physics Experiments, J. Phys. Conf. Ser. **513**, 022010 (2014)
4. S. Agostinelli *et al.* [GEANT4], GEANT4--a simulation toolkit, Nucl. Instrum. Meth. A **506**, 250-303 (2003)
5. R. L. Gluckstern, Uncertainties in track momentum and direction, due to multiple scattering and measurement errors, Nucl. Instrum. Meth. **24**, 381-389 (1963)
6. Z. Drasal and W. Riegler, An extension of the Gluckstern formulae for multiple scattering: Analytic expressions for track parameter resolution using optimum weights, Nucl. Instrum. Meth. A **910**, 127-132 (2018)
7. J. Adam *et al.*, ATHENA detector proposal — a totally hermetic electron nucleus apparatus proposed for IP6 at the Electron-Ion Collider, *JINST* **17** P10019 (2022)
8. ALICE Collaboration, *Letter of Intent for an ALICE ITS Upgrade in LS3,* CERN-LHCC-2019-018 , LHCC-I-034, https://cds.cern.ch/record/2703140/files/LHCC-I-034.pdf
9. W. Snoeys, *et al.,* A process modification for CMOS monolithic active pixel sensors for enhanced depletion, timing performance and radiation tolerance, Nucl. Instrum. Meth. A **871**, 90-96 (2017)
10. ATHENA Twiki, https://wiki.bnl.gov/athena/index.php/Tracking